Article ID: 1006-8775(2011) 04-0352-11

LOCALIZED HADLEY CIRCULATION AND ITS LINKAGE TO PACIFIC SSTA

QIN Yu-jing (秦育婧), WANG Pan-xing (王盘兴)

(Key Laboratory of Meteorological Disaster of Ministry of Education, College of Atmospheric Sciences, Nanjing University of Information Science & Technology, Nanjing 210044 China)

Abstract: The 1979-2001 ERA-40 monthly mean meridional winds are used to calculate the mass streamfunctions in the monsoon region (60–140° E) and Niño zone (160° E–120° W), with which the climate characteristics and intensity variation of the localized Hadley circulation (LHC) are analyzed over the two regions and the linkage of this LHC to Pacific SST is explored. Evidence suggests as follows. 1) The climatological LHC is stronger in the monsoon than in the Niño zone, with its position in the former northward of the latter, especially in the summer half-year. The resulting difference is due mainly to the land-sea heterogeneous distribution and the existence of a cold pool in the equatorial eastern Pacific. 2) The LHC experiences a distinct interannual variability in intensity and during 1979–2001 the LHC strength of the two regions changes broadly in an anti-phase manner. 3) The LHC has its intensity associated closely with Pacific SST in such a way that its strength anomaly in the monsoon (Niño) band in January is correlated negatively (positively) with the SSTA over the all-Niño (1–4) zone (ANZ) in the equatorial middle and eastern Pacific but positively (negatively) correlated to SSTA in the C-shaped area that surrounds the ANZ. The pattern of July is in rough agreement with that of January, except for more feeble correlativity in July, especially over the monsoon region; 4) The ENSO episode has different impacts on the LHC vigor in the two regions. With the occurrence of an El Niño, the LHC is weakened (strengthened) in the monsoon (Niño) region, and the reversal takes place during the La Niña year, with greater anomaly in the Niño area.

Key words: localized Hadley circulation; difference; SST; ENSO

CLC number: P461.2 **Document code:** A **doi:** 10.3969/j.issn.1006-8775.2011.04.005

1 INTRODUCTION

The Hadley circulation (denoted as HC thereafter) refers in general to the meridional circulation in tropics, with its position and intensity season-dependent. Since Hadley[1] published his article concerning the cause of trade wind, the HC has been a topic of scientists because of its importance in atmospheric circulations[2-6]. In the 1960s, scientists discovered big differences in HC at varying meridians, thus proposing a concept of monsoon meridional circulation[7]. In their discussion of the structure of vertical motion in 50° E–130° W in July, Yeh et al.[8] noted that west of 130° E is the SW monsoon zone with the meridional circulations much different from those over the eastern Pacific east of 160° E, and the locally mean circulation, called the localized HC (LHC), exerts great impacts on the regional climate under its control. Liu et al.[9] employed a concept of local meridional circulation to explain the cause of arid climate in the Sahara and NW China, respectively. In comparison to the studies of globally zonal mean HC, little is reported on LHC research, which is limited mainly because it is difficult to use vector techniques to represent the LHC intensity quantitatively, leading to very few studies done of the LHC strength. According to Yue[10], the mass streamfunction (ψ) is employed to denote the LHC, together with the trustworthy 1979–2001 ERA-40 dataset utilized[11-13]. The LHC was investigated in the monsoon zone (60–140° E) and Niño band (160° E–120° W) in order to reveal its climatic characteristics, change in strength and inter-regional

Received 2010-07-16; **Revised** 2011-09-08; **Accepted** 2011-10-15

Foundation item: Natural Science Foundation of China (NSFC, 40975057); The Structure of Tibetan Heat Sources and Oscillation Properties in Conjunction with the Mechanism for the Heat Propagating and Influencing as a key project of the NSFC (40633018); Hadley Circulation Anomaly with Its relation to the Anomaly of Summer Climate in China (E3000008098005)

Biography: QIN Yu-jing, lecturer, Ph.D., primarily undertaking research on atmospheric circulation anomalies and short-term climate prediction.

Corresponding author: QIN Yu-jing, e-mail: qinyujing@nuist.edu.cn

discrepancies.

The LHC is a direct thermal circulation, with its strength in close relationships to SST. Fu[14] compared the Pacific HC between 120–140° W and 140–160° W. It is believed that their difference is related closely to SST at these latitudes. Studies show that in the El Niño summer the global HC is amplified[15, 16] while the LHC is somewhat weakened in the monsoon area[17, 18], with the Pacific SST having obvious effect on atmospheric circulations in East Asia and summer precipitation over eastern China[19, 20]. This work will also deal with the LHC in 60–140° E and 160° E–120° W in relation to Pacific SST, along with the causes addressed.

2 DATA AND METHODS

2.1 *Data*

The dataset used in this work consists of 1) ERA-40[21] monthly mean meridional winds *v* in 1979–2001, totaling 276 months at a horizontal resolution of 2.5° ×2.5° with 23 vertical layers; 2) The SST dataset from Hadley Centre Sea Ice and Sea Surface Temperature data set (HadISST1) at 1º ×1º resolution covering the same length of 1979-2001[22].

2.2 *Methods*

Following Yue[10], the mass stream function for a given longitude is defined as:

$$\frac{a^2\omega\cos\varphi}{g}=-\frac{\partial\psi}{\partial\varphi} \tag{1}$$

$$\frac{a\upsilon_\chi\cos\varphi}{g}=\frac{\partial\psi}{\partial p} \tag{2}$$

From Eq. (2) ψ_i is found for each meridian ($i=1-144$) through a bi-directional linear superimposition scheme[23]. For a particular meridional spacing ($i=a-b$) the area-averaged mass stream function can be found approximately to be of the form

$$[\psi]=\frac{(lonb-lona)\pi}{180}\frac{1}{b-a+1}\sum_{i=a}^{b}\psi_i \tag{3}$$

in which *lona* and *lonb* denote the gridpoints *a*- and *b*- related longitudes, respectively.

2.3 *Regionalization criterion*

Vertical motion inside LHC at 60° E–120° W differs pronouncedly on an interannual basis, and the difference in vertical motion is large between 60–140° E and 160° E–120° W. Wang et al.[24] believed that air-sea interactions over the Indian Ocean and west Pacific (50–170° E) are twofold, i.e., they are affected simultaneously by monsoon and ENSO as opposed to those over the middle eastern Pacific (175° E–80° W) that are under the effect of ENSO alone. After overall consideration the longitude of 150° E is set to be the division by which the zone of 60° E–120° W is separated into a monsoon region in 60–140° E and a Niño band in 160° E–120° W. In order to keep the completeness of the Hadley circulation, the latitude extent covers 60° S–60° N.

3 HC SEASON-DEPENDENT VARIABILITY

For 1979–2001, monthly mean mass streamfunctions, $[\bar{\psi}]$, are computed for the global HC, monsoon band and Niño zone, with the circulation center $\psi>0$ (<0) referred to as a positive (opposite) circulation rotating in a clockwise (counterclockwise) sense.

3.1 *Season-dependent global HC*

Figure 1 depicts monthly global HC patterns in which the bi-hemispheric HC experiences a single cycle annually and when the boreal HC intensifies, the austral HC weakens and vice versa. Furthermore, the northern HC is stronger (weaker) in winter (summer) as opposed to the southern counterpart. Note that the winter and summer are relative to the Northern Hemisphere throughout this article. The austral HC steadily increases from winter to summer, marching northward and during this period the boreal HC gets gradually weakened. In July, hence, the northern (southern) HC is the weakest (strongest), followed by its progressive change for the opposite. However, the global HC development from winter to summer varies from its summer to winter evolution. In January when the boreal HC is strongest, and extends into the Southern Hemisphere only by 10 latitudes compared to the most intense southern HC in July stretching 20 latitudes into the Northern Hemisphere. This is attributed to the fact that the boreal hemisphere is a warn hemisphere, with the yearly-mean heat equator positioned in the Northern Hemisphere. The intensity of austral HC in July being higher than the boreal equivalent in January may be due to the vast expanse of water in the Southern Hemisphere, from which more plentiful vapor is transported in July by the lower-level HC flows, releasing more latent heat via condensation into the ascending arm, thus amplifying the global HC.

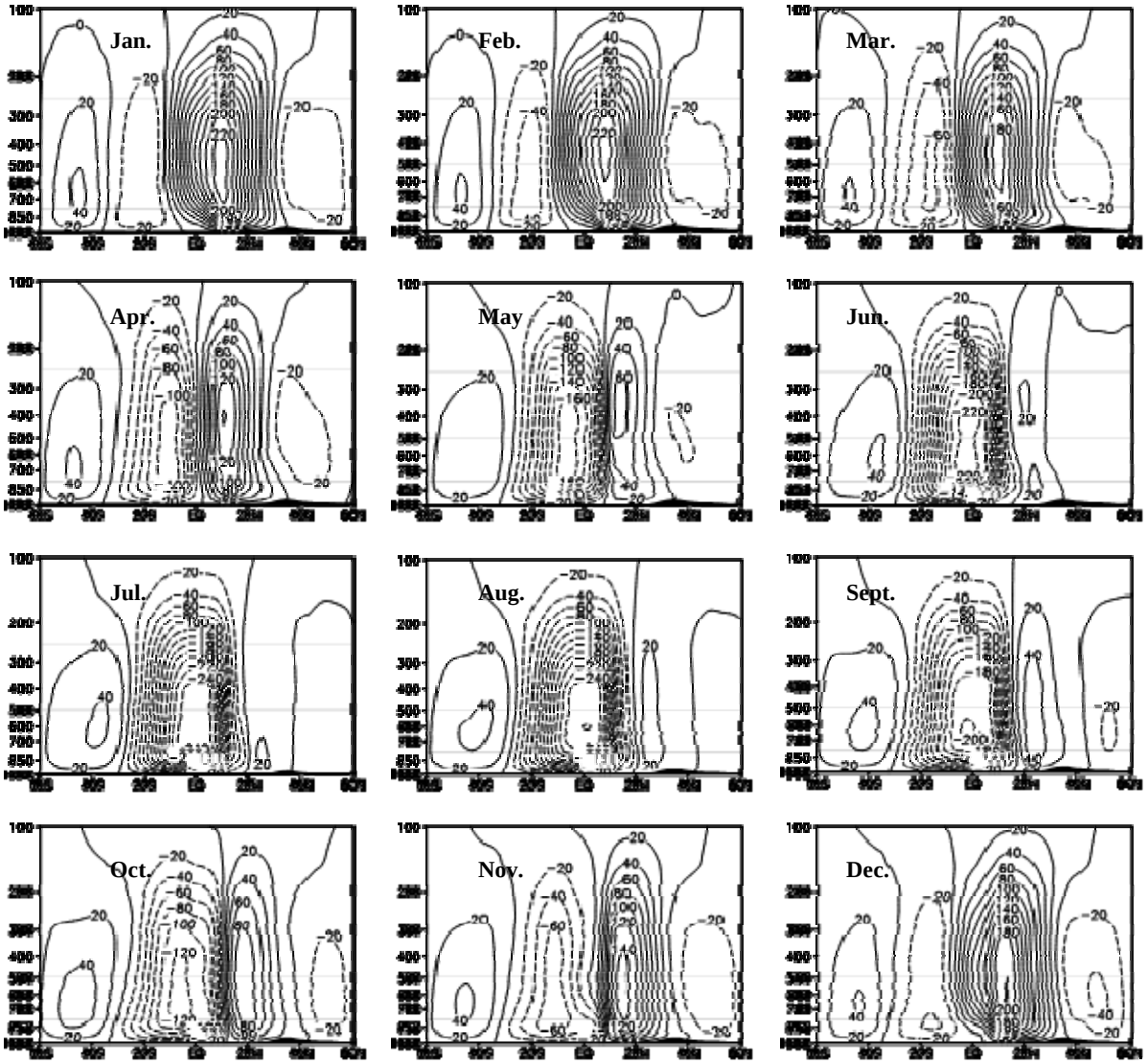

Fig. 1. The 1979-2001 mean monthly global HC. The mass streamfunctions ψ (10^9 kg/s) are designated by contours at intervals of 20 units on the abscissa and pressure (hPa) on the ordinate, with bottom shading for the terrain.

3.2 *LHC seasonal cycle over the monsoon area*

As shown in Fig. 2, the LHC pattern and its evolution in the boreal half-year (October–March) in the monsoon region are similar to those of the global HC except for a closed positive circulation cell (called a new cell hereafter) separated in the mid- and lower-troposphere at 30–40° N in March whereas the April-September pattern differs noticeably from the global HC largely in that the boreal LHC starts reducing rapidly from April, a month ahead of the global HC weakening, and the intensifying new cell replaces the original northern LHC in June–August, occupying the latitudes north of 30° N. This situation differs greatly from that of the global HC. The austral LHC reaches the vicinity of 30° N in July, more northward than the global HC. The Asian continent, its Tibetan Plateau and the Bay of Bengal serve as extensive heat sources in summer[8], where air rises following the thermal adaptation theory. The updraft occurs in nearly all the LHC over the monsoon area at 10° S–35° N in May–September, a region that is broader as compared to that of the global HC.

3.3 *LHC seasonal variation in the Niño belt*

Figure 3 shows that the Niño-zone HC changes are in broad agreement with the global HC except that their positions are further south of the LHC of the monsoon region. From winter to summer the austral LHC develops slowly to the intensity comparable to the boreal LHC in May, one month later than the global HC. The bi-hemispheric LHC stretches into the opposite side by about 10 latitudes at their strongest phase, a situation that is quite symmetric about the equator and due to the homogeneous thermal attribute of the underlying surface in the Niño band. Therefore, the annually averaged heat equator stays in the vicinity of the geographic equator.

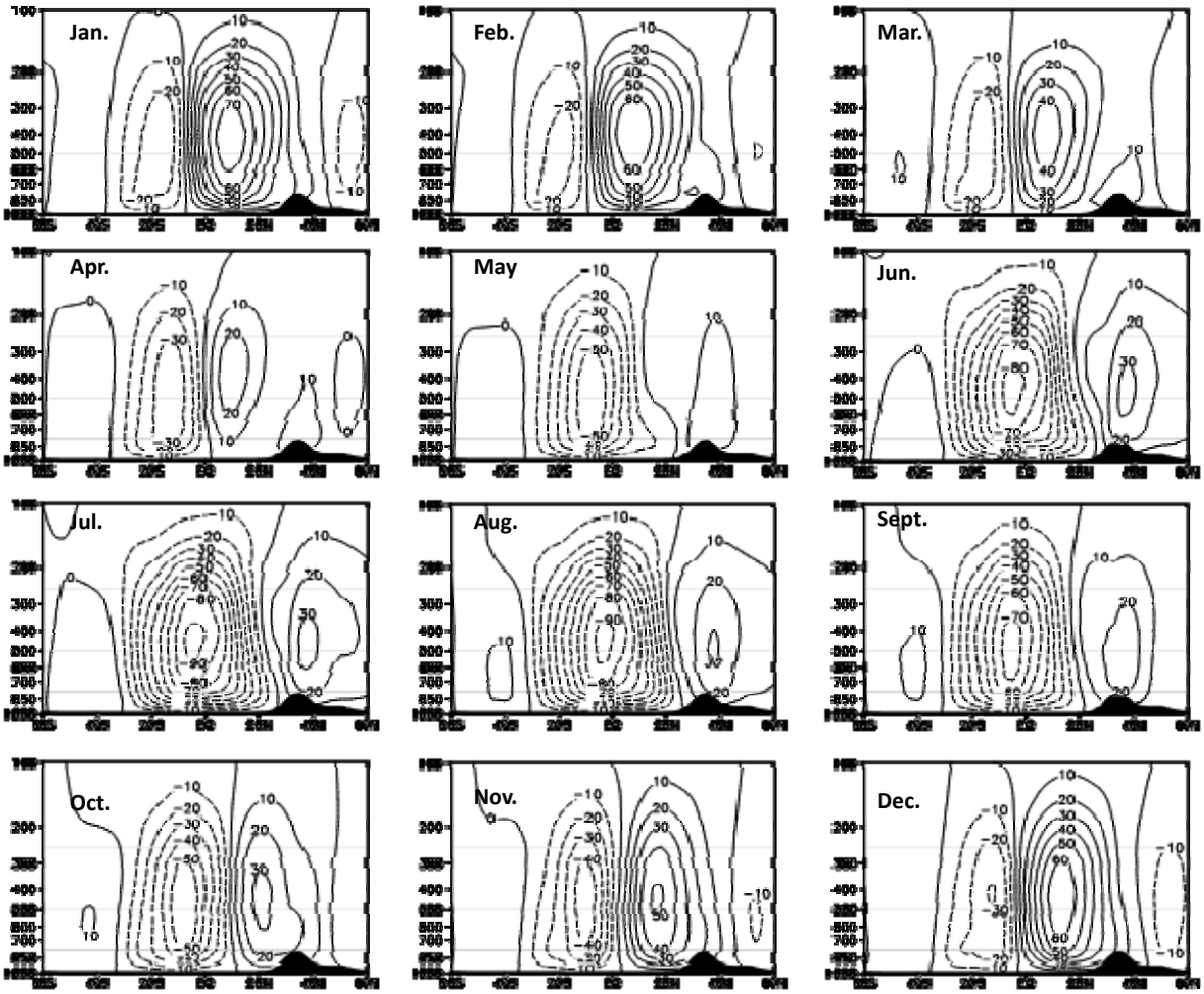

Fig. 2. The 1979-2001 mean monthly LHC patterns over the monsoon region (60–140° E). Otherwise are the same as in Fig.1 except the contours at intervals of 10 units of mass streamfunction.

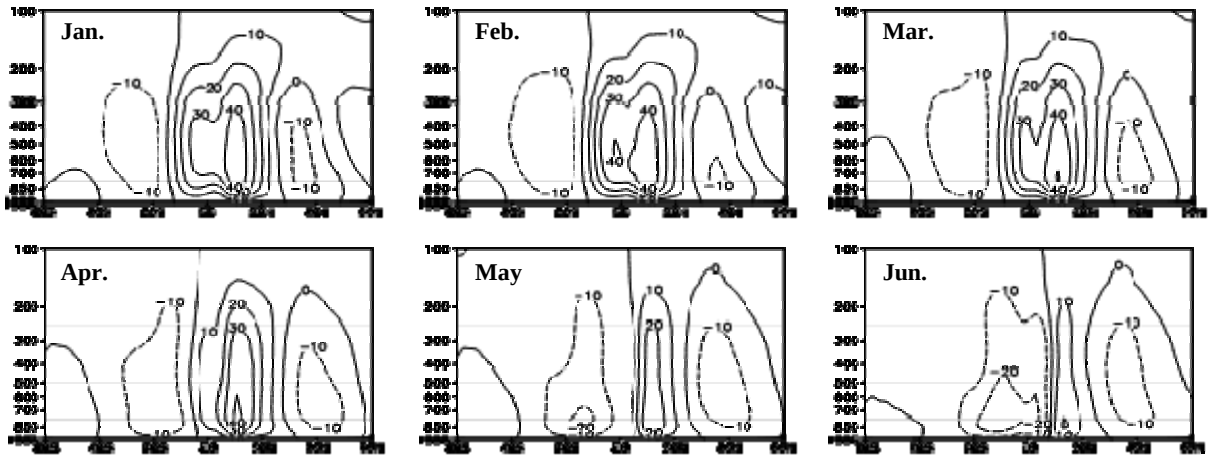

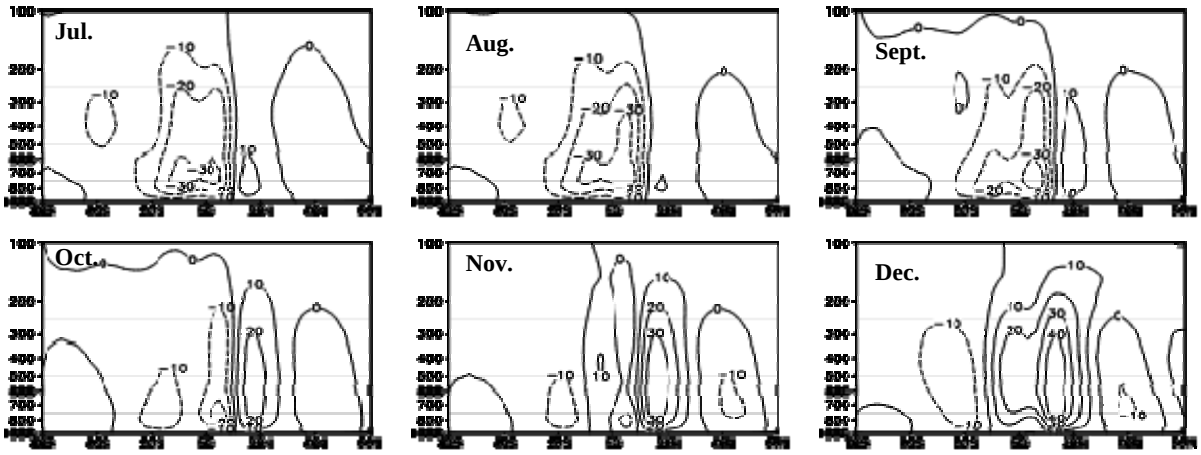

Fig. 3. Same as in Fig. 2 but for the Niño zone (160° E–120° W).

3.4 *Difference in LHC between the monsoon and Niño regions*

From the foregoing analysis we see that the LHC differs greatly between the monsoon and Niño zones. Fig. 4 presents the season-dependent bi-hemispheric LHC cores in the two regions as well as the season- and latitude-dependent 500-hPa zero-value line (denoting the division between the bi-hemispheric HCs). Note that the global HC values thereof are solely for reference. Fig. 4 shows the following three points. 1) The centers of the boreal LHCs in the two study regions are broadly consistent with each other in the winter half-year. In the summer half-year, the northern monsoon-region LHC core is shifted northward, with 37.5° N as the northernmost latitude. The LHC center in the Niño area is south of the monsoon-region LHC core and moves north of 17.5° N at the farthest. In association with the fact that to the north of 20° N is a vast expanse of land for the monsoon region where land-sea thermal contrast causes the land to be warmer than the sea in summer so that the thermal equator moves north and hence the boreal LHC center is positioned more northward than the Niño-zone counterpart. 2) The austral LHC core in the Niño zone is about 10 latitudes south of the equivalent in the monsoon zone except in August–October. But inspection of Figs. 3 and 4b yields that even in August–October the HC as a whole does not move northward except its center. 3) The 500-hPa zero-value line depicts that the Niño-zone HC center is positioned south of the counterpart of the monsoon zone with the exception of November, particularly in the summer half-year.

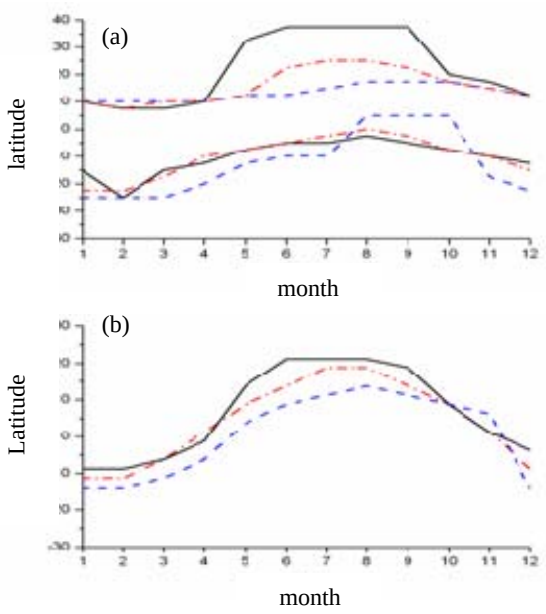

Fig. 4. Latitude-dependent bi-hemispheric HC centers (a) and the latitude-evolving 500-hPa zero-value line (b). The HC in the monsoon (Niño) band is given by the solid (dashed) line and the global HC by the dotted-dashed line.

Table 1 gives the LHC vigor in the monsoon and Niño regions, with SC and NC representing the HC intensity (the biggest absolute values in the centers) in the Southern and Northern Hemispheres, respectively. The change in the intensity stands for the HC seasonal evolution, with CAB (the common ascending branch) designating the difference (northern minus southern) in the strength of a LHC rising arm between the two hemispheres that is well indicative of the strength of the HC as a whole. It is seen that the southern LHC is stronger in the monsoon region than in the Niño area throughout the year, with the annual mean value being more than twice that of the latter while except in March–May, the northern HC intensity is higher in the monsoon region than in the Niño area, particularly during June–September, due to the fact that the boreal LHC over the monsoon zone rapidly weakens in April

such that LHC in the spring, as the transition between winter and summer, is weaker than that of the Niño area. In summer the northern new cell in the monsoon region is much stronger than the boreal LHC in the Niño zone. Except in March–April, the CAB is more vigorous over the monsoon region than in the Niño area, resulting in a yearly difference of 41.5 units of 10^9 kg/s.

Table 1. Bi-hemispheric LHC intensity in the monsoon zone versus the Niño region. Units: 10^9 kg/s.

month	Monsoon zone			Niño zone		
	SC	NC	CC	SC	NC	CC
Jan.	27.3	77.8	105.1	16.5	47.4	63.8
Feb.	23.7	69.7	93.4	19.4	48.2	67.7
Mar.	25.4	47.3	72.6	17.2	50.3	67.6
Apr.	37.3	27.3	64.6	18.9	42.0	60.9
May	57.4	19.6	77.0	22.1	27.8	50.0
Jun.	83.6	33.0	116.6	28.2	21.2	49.4
Jul.	92.8	33.7	126.4	33.1	14.4	47.5
Aug.	93.5	31.3	124.9	38.8	11.0	49.8
Sept.	74.8	27.1	101.9	37.0	14.1	51.0
Oct.	58.5	32.5	91.1	25.0	24.4	49.5
Nov.	45.8	50.9	96.7	14.5	36.4	50.9
Dec.	30.9	67.9	98.8	15.7	47.2	62.9
year m.	54.2	43.2	97.4	23.9	32.0	55.9

On the whole, the LHC is stronger and the center is more northward in the monsoon region than in the Niño zone. Studies[25-26] suggested that the location of the HC rising leg depends strongly on underlying surface temperature, and the HC vigor is dependent dominantly upon the meridional temperature gradient (i.e., the temperature difference between the vicinity of the thermal equator and higher latitudes) and vapor convergence is related to subtropical evaporation caused by low-level HC flows. As shown in Figs. 2 and 3, north (south) of 20° N in the monsoon region is land (sea) but practically no land is in the Niño zone. The land-sea thermal contrast plays its role as follows: In the winter half-year temperature is lower on land than over sea at the same latitude, resulting in bigger meridional temperature gradient in the monsoon region than in the Niño zone so that the LHC is more intense in the former, whereas in the summer half-year land is warmer, shifting the thermal equator more northward in the monsoon region than in the Niño zone. With the Tibetan Plateau thermal effect included, the above factors lead to distinct LHC properties between the two study regions in summer. Consequently, the land-sea geographic distribution is believed to be the main cause of the vast discrepancy in the LHC between the areas. In winter (summer), additionally, the existence of an equatorial eastern Pacific cool pool weakens the meridional temperature gradient (and the southern subtropical evaporation) in the Niño zone, which also serves as a principal cause of the weaker LHC there.

4 LOCALIZED HC INTENSITY CHANGE IN ASSOCIATION WITH PACIFIC SST

4.1 *Change in LHC Strength*

The LHC intensity index is based on the strength of CAB. Three points are noted in Fig. 5. 1) These LHC intensities experience noticeable variation on the interannual basis. 2) With the intensities being comparable in both the project regions except April, the LHC strengths are weaker in the other months of the years in the Niño band. 3) The El Niño year corresponds broadly to the valley (peak) LHC value in the monsoon (Niño) region, especially Januaries of 1983, 1992 and 1998. The LHC is stronger in the Niño band than in the monsoon region, thereby demonstrating that the LHC is intensified (weakened) in the former (latter) case during the El Niño episode. The reversal happens in the La Niña year, thus indicating that the ENSO cycle bears a close relation to the LHC vigor, differing in effect for the two zones.

Examination of Fig. 5 and Table 2 yields that the LHC strength varies roughly oppositely in phase between the monsoon and Niño regions, and the correlation coefficients are negative except the values for April, July and August that are very small positive magnitudes and fail to be statistically significant at the 0.1 level, and the negative correlation coefficients for January, May and November are significant at the 0.05 level. The anti-correlation feature is thought to be associated with the ENSO cycle.

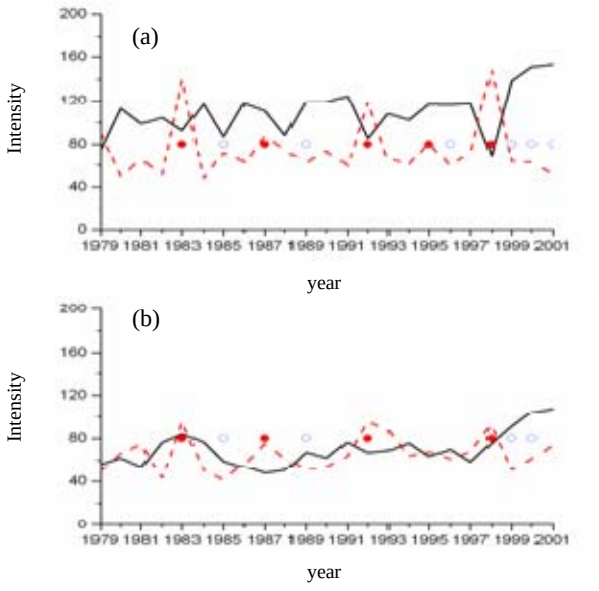

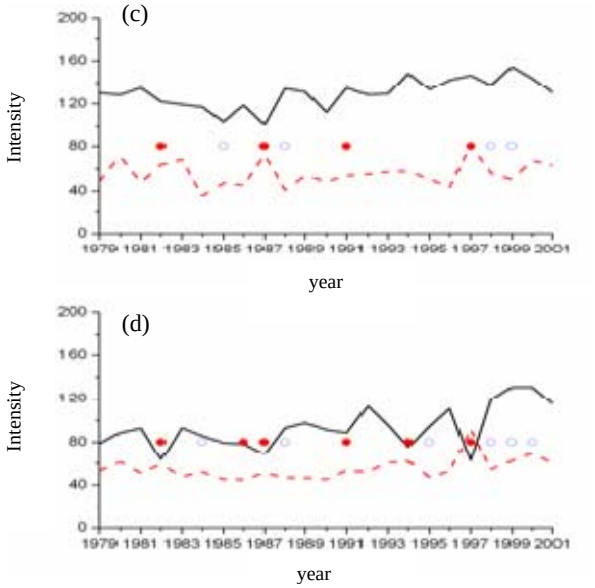

Fig. 5. Variation in LHC intensity, with the change in the monsoon (Niño) zone denoted by full (dashed) line. Penal (a) is for January, (b) for April, (c) for July and (d) for October, with solid (open) dots designating an El Niño (La Niña) event.

Table 2. Correlation coefficients between the monsoon and Niño area LHC strengths.

Month	Correlation coefficients
Jan.	**-0.63**
Feb.	-0.29
Mar.	-0.30
Apr	0.09
May	**-0.45**
Jun.	-0.38
Jul.	0.09
Aug.	0.32
Sept.	-0.18
Oct.	-0.03
Nov.	**-0.43**
Dec.	-0.40

4.2 *Time lagged correlation between LHC intensity anomaly and SSTA*

Correlation coefficients are calculated between LHC strength anomaly and Pacific SSTA values six months ahead and lagging behind in the two study regions in January and July (Figs. 6 and 7 give the simultaneous correlation pattern), revealing that the correlative patterns are steady and coefficients are large.

In January, the LHC vigor index of the monsoon (Niño) area is in negative (positive) correlation with SST over the ANZ (which refers to the all-Niño zone consisting of Niño areas 1 through 4 in the equatorial central eastern Pacific) but in positive (negative) correlativity with SST in the C-shaped band surrounding the ANZ. The LHC intensity anomaly of the monsoon region has the strongest correlation with SSTA three months in advance, with the LHC intensity anomaly correlated to ahead-of-time and simultaneous SSTA being superior to their lagging correlativity and the synchronous correlation being the most intense in the Niño zone. The LHC vigor anomaly-SSTA correlation pattern in January in the monsoon region is analogous to that of the components reconstructed based on central-western Pacific meridional convergence data with SST[27] and the LHC ascending arm intensity can characterize, to some degree, the mass convergence strength in the meridional direction in the western Pacific region. As a result, the January monsoon-zone LHC vigor index correlated with the Pacific SST is likely to bear a close relation to meridional wind convergence there.

In July, the January pattern of correlation between LHC anomaly of the monsoon zone and SSTA barely maintained, during which the C-shaped area shows positive correlativity, with the coefficient being slightly smaller than that of January. But the negative correlation coefficients become very small in the mid-eastern Pacific, with the values only in a few zones thereof being statistically significant at the 0.05 level. The correlation pattern between LHC anomaly of the Niño band and SSTA in July is similar to that of January, just with weaker correlation in the C-shaped area, and the synchronous correlation in July is the strongest. In addition, the lagged correlation of July is superior to the LHC correlation to SST in advance. This illustrates that during an El Niño event the Niño-zone LHC intensifies and imposes strong positive feedback on mid-eastern Pacific SST that persists for more than five months.

The Pacific SSTA pattern in the ENSO episode, particularly its mature phase, is contrary to the SSTA pattern in the ANZ and the C-shaped area[28], just in conformity with the pattern of LHC correlated to the Pacific SST. This demonstrates that the LHC intensity is closely associated with the ENSO event in both the study regions, with their stronger correlativity in January than in July. Lan et al.[29] noted that the interannual variation in the Pacific atmospheric heat sources and vapor sinks bears a close relation to the ENSO cycle, which may be one of the causes of ENSO-produced LHC anomaly.

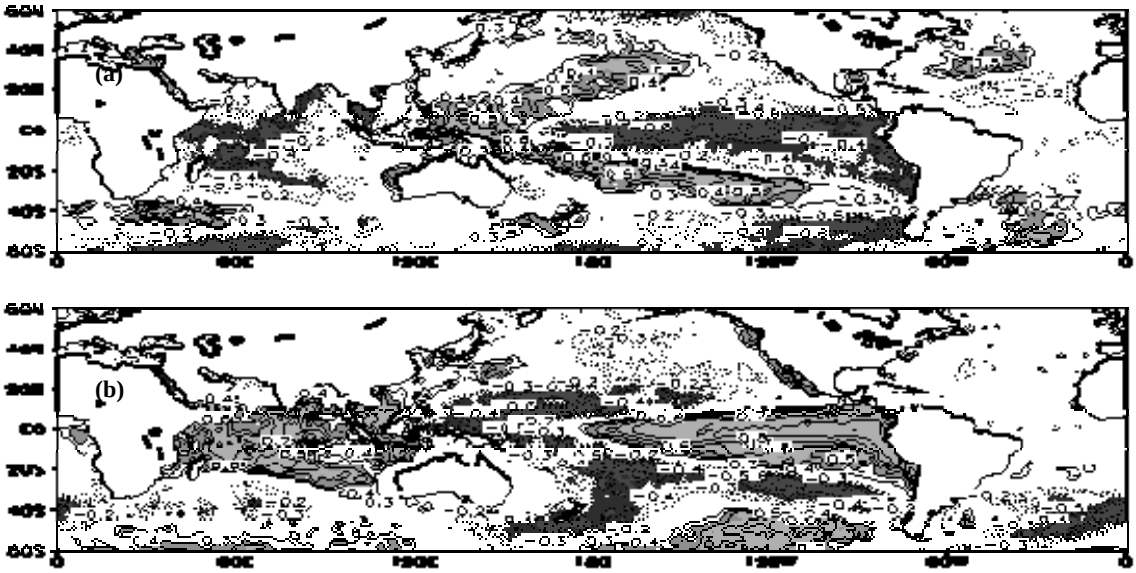

Fig. 6. The simultaneous correlation pattern between LHC intensity anomaly and SSTA in January, with the monsoon zone in (a) and Niño region in (b), and the shading denotes that the values are statistically significant at the 0.05 level.

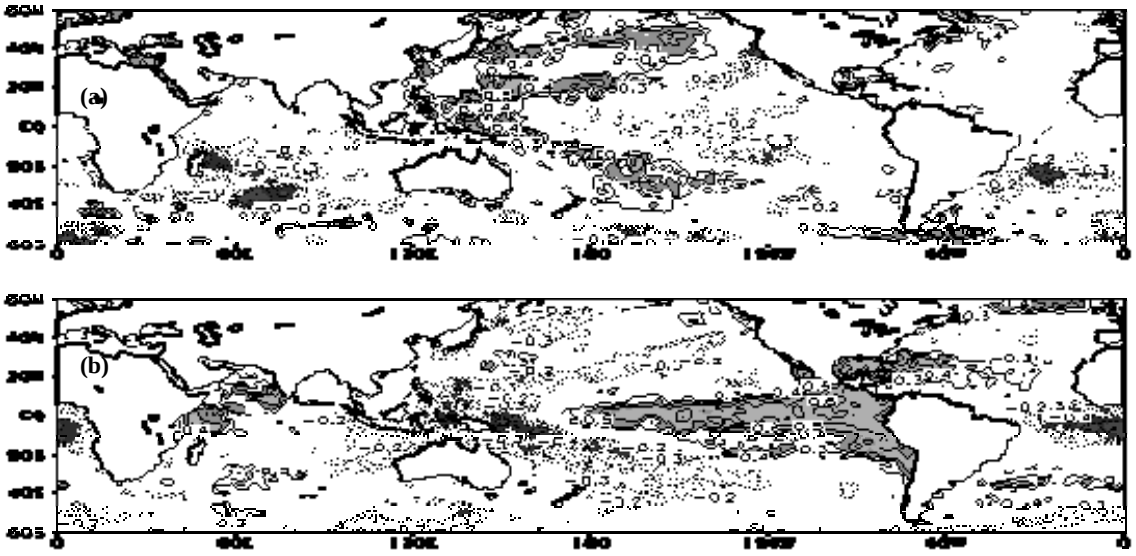

Fig. 7. Same as Fig. 6 except for July.

4.3 *Composite analysis of LHC intensities*

According to the Niño indices over Niño 3.4[30], mature El Niño phases in January are chosen for 1964, 1966, 1969, 1973, 1977, 1978, 1983, 1987, 1992, 1995 and 1998; the El Niño starting to develop in July are chosen for 1963, 1965, 1972, 1982, 1987, 1991, 1994 and 1997; the mature La Niña stage in January are selected for 1965, 1968, 1971, 1974, 1976, 1985, 1989, 1996, 1999, 2000 and 2001; the La Niña event starting to develop in July are chosen for 1964, 1970, 1971, 1973, 1975, 1988, 1998 and 1999. To guarantee the required number of samples the data time has been advanced to 1962. Later, a composite analysis is performed of the LHC indices in ENSO cold/warm phases in January and July over the monsoon and Niño regions.

Figures 8, 9a and 9b show that during January as the mature phase of the El Niño episode there shows an abnormal opposite (positive) circulation north (south) of 10° N in the monsoon region, indicative of a weakening LHC there. In the Niño zone, however, an anomalous positive (opposite) circulation is present in the Northern (Southern) Hemisphere, indicating the enhanced LHC there that is moved north as a whole. In January during the mature phase of the La Niña event the anomalous circulation pattern is broadly contrary to that of January for El Niño episodes over the two study regions, with an intensified (weakened) LHC in the monsoon (Niño) zone, and the LHC moved south as a whole.

It is seen from Figs. 8c, 8d, 9c, and 9d that for the

El Niño phase in July over the monsoon area an abnormal opposite (positive) circulation shows up north (south) of 10° S, suggestive of the austral LHC center being displaced northward, and a weakened LHC in the Northern Hemisphere. For the La Niña stage in July an anomalous positive (opposite) circulation appears north (south) of 10° S, indicating that the northern LHC intensifies. From part of the correlation analysis we see that the LHC over the monsoon region has a mildly negative correlation to the ANZ SST in July but the anomalous LHC intensity in July is comparable to that of January, thus demonstrating that the ENSO impacts on LHC in the monsoon region may be dominantly through SSTA in the C-shaped area. For the El Niño phase in July in the Niño zone there is an abnormal positive (opposite) circulation in the Northern (Southern) Hemisphere, suggestive of a reinforced LHC. Reversal happens in the July phase of the La Niña event. The anomalous circulation over the Niño zone is not as intense in July as in January, illustrating that the ENSO effect on the Niño-band LHC is weaker in July than in January.

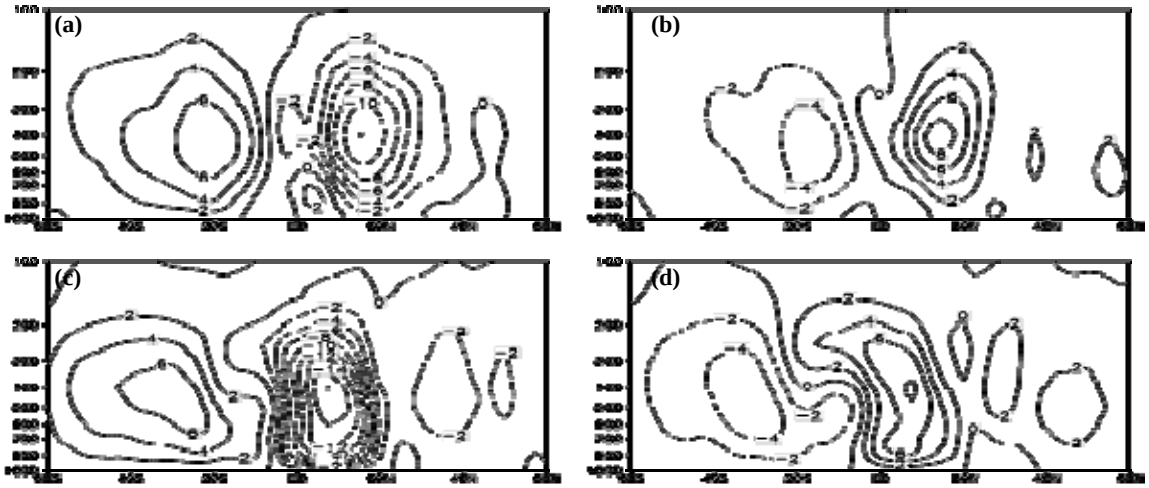

Fig. 8. Composite LHC patterns during ENSO events in the monsoon region, with the El Niño phase in January (a), La Niña phase in January (b), El Niño phase in July (c) and La Niña phase in July (d).

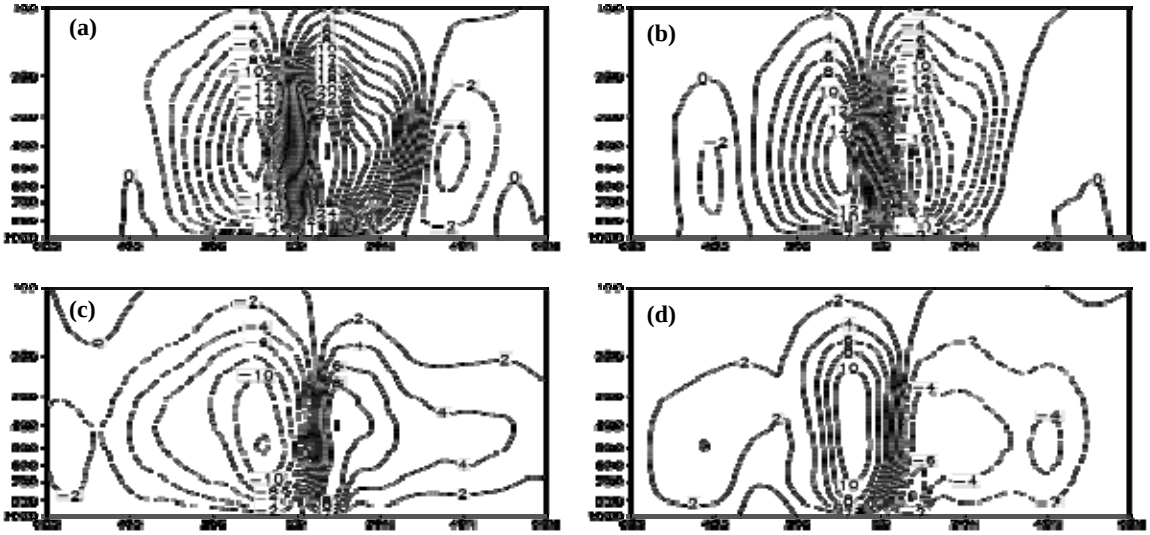

Fig. 9. Same as in Fig. 8 except in the Niño zone.

To sum up, the ENSO exerts contrary impacts on the LHC strength in the two project areas. When the El Niño phenomenon occurs, the LHC is weakened (amplified) in the monsoon (Niño) area. Contrary is the case for the La Niña episode. With the El Niño happening, positive SSTA is over the middle-eastern Pacific in contrast to negative SSTA in the C-shaped area[28], reducing (strengthening) the meridional temperature gradient over the monsoon (Niño) region, leading to weakened (invigorated) LHC in the monsoon (Niño) region. Reversal occurs when the La Niña happens. The asymmetry in intensity of the ENSO cycle[31] means that the La Niña episode is weaker compared to the El Niño event and thus the former is not as strong as the latter with regard to the effect on the LHC. Besides, ENSO cycles influence the Niño-area LHC more strongly than the LHC in the monsoon region both in January and July (with the

anomalous circulation being stronger in the Niño region than over the monsoon region, but the HC itself being feeble). This is associated with larger ENSO-caused change in the Niño-area meridional temperature gradient (with the middle-eastern Pacific SST changes being the most obvious) and also with Pacific-Indian Ocean air-sea interactions under the effect of monsoon and ENSO and the eastern Pacific (175° E–80° W) interactions just under the ENSO impact[24].

5 CONCLUDING REMARKS

The 1979-2001 ERA-40 monthly meridional winds are used to calculate mass streamfunction in the monsoon and Niño zones, with which LHC climate attributes and intensity change there as well as the relation of LHC strength to Pacific SST are investigated. Evidence suggests as follows.

1) The climatology of LHC is stronger in the monsoon than over the Niño area, with the circulation positioned farther north in the former case, particularly in the summer half-years. This is attributed mainly by the heterogeneous land-sea distribution and the role of the equatorial eastern Pacific cool pool.

2) Noticeable interannual variation happens to the LHC intensity, with its strength varying in a broadly opposite manner in the two zones over 1979–2001.

3) LHC vigor depends strongly on the Pacific SST in such a way that in January the LHC intensity of the monsoon (Niño) region is in negative (positive) correlation to the equatorial mid-eastern Pacific ANZ SST and in positive (negative) correlation to the SST in the C-shaped area surrounding ANZ. The correlation pattern in July is roughly similar to that in January except that the negative correlation is weaker than that in January, especially in the monsoon band.

4) The ENSO event has a different effect on LHC intensity in both the regions, i.e., when the El Niño episode the LHC is weakened (reinforced) over the monsoon (Niño) region. Just contrary is the case of the La Niña event and with an extremely significant anomaly in the Niño zone, when the ENSO cycle influences the LHC vigor by altering the meridional temperature gradient.

5) A great discrepancy exists in the LHC intensity between the two study regions, with the circulation pattern and strength changes different from those of the global HC, a problem that is of much importance in studies on regional climate.

Acknowledgement: The data are provided by Nanjing Atmospheric Data Service, Geoscience Division of the National Natural Science Foundation of China. The authors are also grateful to ECMWF and the Hadley Centre of UK Met Office for their original data.

REFERENCES:

[1] HADLEY G. Concerning the cause of the general trade-wind [J]. Phil. Trans., 1735, 29: 58-62.
[2] DIMA M I, WALLACE M J. On the seasonality of the Hadley cell [J]. J. Atmos. Sci., 2003, 60 (12): 1522-1526.
[3] LORENZ E N. The nature and theory of the general circulation of the atmosphere [M]. Tech. Doc. 218, World Meteorological Organization, Geneva, 1967: 161pp.
[4] WU Guo-xiong, TIBALDI S. Effect of mechanical forcing on the meridional circulation and transfer properties of the atmosphere [J]. Adv. Atmos. Sci., 1987, 4(1): 24-42.
[5] WU Guo-xiong, LIU Yi-min, REN Rong-cai, et al. Relation of a steady subtropical high to vertical motion [J]. Acta Meteor. Sinica (in Chinese), 2004, 62(5): 587-597.
[6] OORT A H, PEIXOTO J P. Global angular momentum and energy balance requirements from observations[M]// Adv. Geophys., New York: Academic Press,1983: 355-490.
[7] YANG Jin-xi. Northern mean meridional circulation and monsoon meridional circulation [M]// Collection of Geographic Papers (in Chinese). Beijing: China Scientific Press, 1965.
[8] YEH Tu-cheng, YANG Guang-ji, WANG Xing-dong. Mean vertical circulation over Eastern Asian and the Pacific. Part I: Summer [J]. Chin. J. Atmos. Sci., 1979, 3(1): 1-11.
[9] LIU P, WU G, SUN S. Local meridional circulation and deserts [J]. Adv. Atmos. Sci., 2001, 18(5): 864-872.
[10] YUE Yang. On Interannual variation of summer monsoon meridional circulation in eastern Asia and atmospheric responses to dipole-type SST forcing over the Indian Ocean [D]. Nanjing: MS thesis at Nanjing University of Information Sci. & Tech. (in Chinese), 2007.
[11] BROMWICH D H, FOGT R L. Strong trends in the skill of the ERO-40 and NCEP-NCAR reanalyses in the high and midlatitudes of the Southern Hemisphere 1958-2001 [J]. J. Climate, 2004, 17(23): 4603-4619.
[12] TRENBERTH K E, STEPANIAK D P, HURRELL J W. Quality of reanalyses in the tropics [J]. J. Climate, 2001, 14(7): 1499-1510.
[13] STERL A. On the (In) Homogeneity of reanalysis products [J]. J. Climate, 2004, 17(19): 3866- 3873.
[14] FU Cong-bing. The change in the pattern of mean meridional circulation and long-term weather process [J]. Acta Meteor. Sinica (in Chinese), 1979, 37(1): 74-85.
[15] WU Guo-xiong, CUBASCH U. El Niño-related SSTA influencing zonal mean meridional circulation and atmospheric transfer properties [J]. Sci. China (in Chinese), 1986, 15(10): 1109-1120.
[16] CHENG Ya-jun, WANG Pan-xing, LI Li-ping. Diagnosis of low-latitude mean meridional circulation anomalies in relation to SSTA [J]. J. Trop. Meteor. (in Chinese), 2002, 18(3): 193-202.
[17] CHEN Yue-juan, ZHOU Ren-jun, JIAN Jun. Relation of Eastern-Asian summer monsoon circulation to ENSO cycle [J]. Plateau Meteor. (in Chinese), 2002, 21(6): 537-545.
[18] WANG Pan-xing, XU Jian-jun, XU Ying-long. Seasonal variation in circulation over the monsoon region in relation to its anomaly during an El Niño episode [J]. Quart. J. Appl. Meteor. (in Chinese), 1995, 6(4): 407-413.
[19] PENG Jia-yi, SUN Zhao-bo. Springtime SSTA over the equatorial eastern Pacific impinging upon spring – summer evolution of eastern Asian atmospheric circulation [J]. J. Trop. Meteor (in Chinese). 2001, 17(4): 398-404.
[20] YU Zhen-shou, SUN Zhao-bo, ZENG Gang. Effect of Pacific SSTA upon summer precipitation over eastern China. Part II: Numerical experiment [J]. J. Trop. Meteor. (in Chinese),

2005, 21(5): 478-487.
[21] SIMMONS A J, GIBSON J K. The ERA-40 project plan [R]// ERA-40 project plan report series No. 1., Reading: ECMWF, 2000: 1-62.
[22] RAYNER N A, PARKER D E. Global analyses of sea surface temperature, sea ice and night marine temperature since the late nineteenth century [J]. J. Geophys. Res., 2003, 108(D14): 4407.
[23] QIN Yu-jing, WANG Pan-xing, GUAN Zhao-yong et al. Comparison of the Hadley cells calculated from two reanalysis data sets [J]. Chin. Sci. Bull., 2006, 51(14): 1741-1746.
[24] WANG P, HE J, GUO P, et al. Regional differences of tempo-spatial characteristics of air-sea interactions in tropical oceans [J]. Acta Meteor. Sinica, 2001, 15(4): 407-419.
[25] TRENBERTH K E, STEPANIAK D P. Seamless poleward atmospheric energy transports and implications for the Hadley circulation [J]. J. Climate, 2003, 16(22): 3706-3722.
[26] DUAN An-min, LIU Yi-min, WU Guo-xiong. April-June Tibetan heat regime related to the mid-summer anomalies of eastern Asian precipitation and atmospheric circulation [J]. Sci. China (D ser.) (in Chinese), 2003, 33(10): 997-1004.
[27] ZHANG Zu-qiang, DING Yi-hui, ZHAO Zong-ci et al. Interannual variation in tropical Pacific meridional wind anomalies in relation to SSTA [J]. J. Trop. Meteor. (in Chinese), 2002, 18(2): 111-120.
[28] WALLACE J M, RASMUSSON E M, MITCHELL T P et al. On the structure and evolution of ENSO-related climate variability in the tropical Pacific: Lessons from TOGA [J]. J. Geophys. Res., 1998, 103(C7): 14241-14259.
[29] LAN Guang-dong, WEN Zhi-ping, HE Hai-yan. Interannual variability of atmospheric heat sources and vapor sinks over the tropical Pacific and its linkage to SSTA [J]. J. Trop. Meteor. (in Chinese), 2004, 20(3): 259-270.
[30] Climate Prediction Center, National Weather Service (USA). Cold and Warm Episodes by Season [EB/OL]. (2008-08-08) [2010-07-16] http://www.cpc.ncep.noaa.gov/products/analysis_monitoring/ensostuff/ensoyears.shtml
[31] LI Chong-yin, MU Mu, ZHOU Guang-qing. Mechanism and prediction studies of the ENSO [J]. Chin. J. Atmos. Sci., 2008, 32(4): 766-781.

Citation: QIN Yu-jing and WANG Pan-xing. Localized Hadley circulation and its linkage to Pacific SSTA. *J. Trop. Meteor.*, 2011, 17(4): 352-362.